



STUDIES ON GROWTH AND PHYSICAL PROPERTIES OF PIPERAZINIUM NITRATE SEMI ORGANIC SINGLE CRYSTAL

S. Sivapriya¹, K. Balasubramanian^{2*}

Article History: Received: 12.12.2022

Revised: 29.01.2023

Accepted: 15.03.2023

Abstract

Piperazinium-Nitrate (PPN) single crystal was grown by slow evaporation technique. The grown crystal structure was determined from single crystal X-ray diffraction studies. The mode of vibration and functional group present in the grown crystal were identified by FTIR analysis. The linear optical properties of PPN crystal were studied from uv-vis spectrum. Vickers microhardness testing was carried out on the as grown crystal surface to reveal the mechanical properties of the crystal. TG-DTA analysis shows that the crystal has no phase transformation before its melting point. The Laser damaged threshold value of grown crystal has been measured using Nd:YAG laser with the wavelength of 1064nm. Third order non linear optical property of the grown crystal was studied by Z-Scan technique.

^{1,2*}Research scholar Reg.NO.12122. PG and Research Department of Physics, The MDT Hindu College, Tirunelveli-627006, TamilNadu, India. (Affiliated to Manonmanium Sundaranar University, Abishekapatti, Tirunelveli, 627 012, Tamilnadu, India)

DOI: 10.31838/ecb/2023.12.s2.067

1. Introduction

Nowadays, the researchers are interest to grow NLO crystals because of their demands in electronic industries. The ultimate aim of the researcher has to develop new NLO crystals have low refractive index, low dielectric constant, synthetic flexibility, quick reaction times, and are simple to fabricate into devices.[1-3]. After the discovery of the laser and the consequent demonstration of quartz harmonic generation, non linear optics has emerged as an active research field [4] In solid state technology the application of NLO materials are telecommunications, , image processing, harmonic generators, optical computing, laser lithography sensors, diode lasers etc.[5]. The development of new materials has directed to the synthesis of many semi organic materials. The semi organic materials have large nonlinearity, high resistance laser induced damage and low angular sensitivity [6-8]. In this present work the organic compound of Piperazine mixed with nitric acid to form Piperazinium nitrate (PPN). The crystal of Piperazinium nitrate was built up from singly protonated piperazinium residues and nitrate anions. A three-dimensional structure is

created by the hydrogen bonds connecting the elements. Both donor and acceptor groups are typically present in efficient materials, and substantial p-delocalization has been identified as a factor contributing to large third order nonlinearities [9]. In the present work, we have made efforts to grow crystal of piperazinium nitrate (PPN) by slow evaporation solution growth method. The grown crystals were characterized by single crystal XRD, Fourier transform infrared, UV-Vis NIR spectroscopy, TG-DTA, Vickers micro hardness, dielectrics and Third order nonlinear optical studies.

Experimental procedure

The slow evaporation method is used to grow Piperazinium Nitrate (PPN) single crystals. The Equimolar ratio of piperazine and Nitric acid was dissolved in distilled water, then using magnetic stirrer, the solution stirred constantly for 3 hrs. The prepared saturated solution was filtered using whatman filter paper. The filtered solution was kept undisturbed at room temperature for slow evaporation. The single crystal of PPN was harvested in a span of twenty days. The grown crystals were shown in Fig.1.

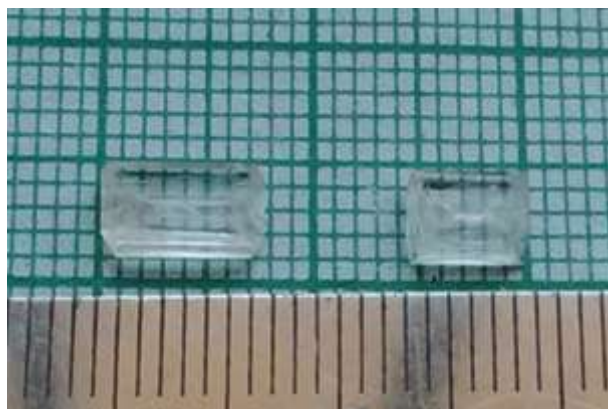


Fig.1 As grown PPN single crystal

2. Result and discussions

Single crystal XRD:

The single crystal X-ray diffraction (SXRD) SXRD was used to analyze the grown PPN crystal in order to determine the lattice parameter values. The grown PPN single crystal belongs to monoclinic

system with space group $p2_1/c$. The obtained values of lattice parameter are $a = 4.65(3)\text{\AA}$, $b = 12.40(5)\text{\AA}$, $c = 12.24(7)\text{\AA}$, $\alpha = \gamma = 90^\circ$ and $\beta = 95.62^\circ$. The volume is $V = 728.9\text{\AA}^3$. The obtained values are good agreement with the reported value [10] (Genivaldo Julio Perpe'tuo et al., 2005). The values are tabulated in table.1

Table.1 crystallographic data of PPN crystal.

Cell parameters	PPN	Reported values
Crystal system	Monoclinic	Monoclinic
Space group	P21/c	P21/c
Unit cell dimension	$a=4.65(3)\text{\AA}$	$a = 4.44(9)\text{\AA}$
	$b = 12.40(5)\text{\AA}$	$b = 12.95(3)\text{\AA}$
	$c = 12.24(7)\text{\AA}$	$c = 12.67(3)\text{\AA}$
	$\alpha = \gamma = 90^\circ$	$\alpha = \gamma = 90^\circ$
	$\beta = 93.62^\circ$	$\beta = 95.62^\circ$

Volume	$V = 704.3 \text{ \AA}^3$	$V = 725.9 \text{ \AA}^3$
--------	---------------------------	---------------------------

FTIR Spectral Analysis

The SHIMADZU IR AFFINITY 1S spectrometer is used to recorded the FTIR spectrum of grown PPN single crystal with the frequency range from

400 cm^{-1} to 4000 cm^{-1} . The FTIR spectrum of PPN crystal shows the presence of functional group in the crystal. The FTIR spectrum of grown PPN crystal is shown in fig.2.

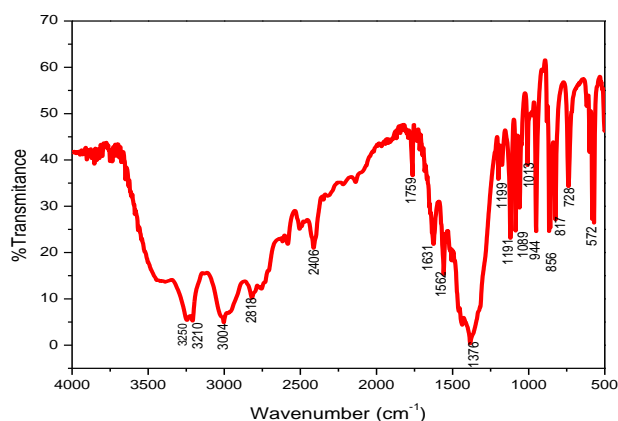


Fig.2 FTIR spectrum of PPN

The band observed at from 3250 cm^{-1} to 3200 cm^{-1} is due to OH stretching vibration. The C-H-Stretching vibration was observed in the band at 2818 cm^{-1} . The peak at 1560 cm^{-1} is due to the presence of aliphatic nitro compounds (N-H). The broad observed band at 1378 cm^{-1} indicates the presence of nitrate ions in the crystal. the peak observed in the range of 1190 cm^{-1} which is due to the presence of C-N stretching vibration. The aromatic C-H-out of plane bending vibration was

found at the peak of 944 cm^{-1} . The medium absorption between 850 and 670 cm^{-1} is due to C-H bending vibration [11].

UV-Vis Spectral analysis

The optical absorption and transparency of grown PPN single crystal has been recorded using SHIMADZU SPECTROMETER UV-1800 in the range of 200nm-1100nm. The UV-Vis spectrum of PPN as shown in Fig.3.

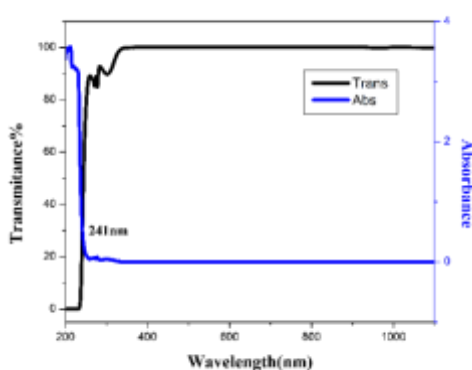


Fig.3 UV- Spectrum of PPN

The grown PPN single crystal has highly transparent throughout the visible region. The UV cut off wavelength of the PPN crystal was found to be 241nm. The absorption coefficient (α) was calculated from the spectrum using following relation

$$\alpha = (2.303/t) \log (1/T) \quad (1)$$

where T is transmittance(%) and "t" is the thickness of the crystal. The band gap energy can be calculated using the value of absorption coefficient. According to Tauc et al., 1996 , The optical band gap (E_g) was estimated using the following relation [12].

$$\alpha h\nu = A (h\nu - E_g)^n \quad (2)$$

the plotted curve between $(\alpha h\nu)^{1/2}$ and photon energy ($h\nu$) shows linear behavior which can be shown in Fig.4. The optical energy band gap (E_g) is calculated by extrapolating the linear component of the curve to the point where $(\alpha h\nu)^{1/2} = 0$. By using this technique, it was discovered that the formed crystal's optical band gap was 5.14 eV. By

theoretical calculation of band gap energy using the relation $E_g = hc/\lambda$ the optical band gap energy was found to be 5.1eV. From UV spectrum the grown PPN single crystal has wide transparency throughout the visible region, which is important for NLO applications.

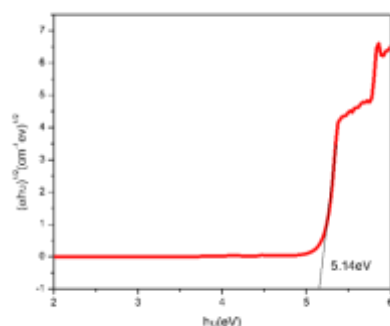
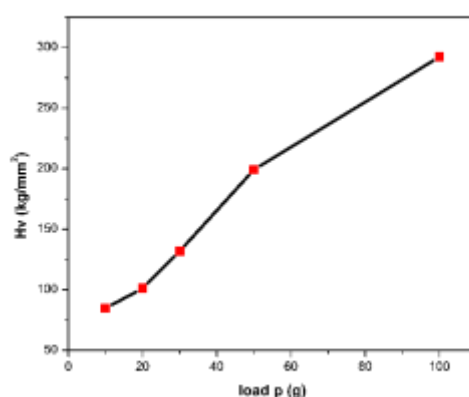


Fig.4 Tauc plot of PPN

Micro hardness studies:

The efficiency of crystalline materials is mostly governed by their mechanical qualities, which are generally linked to their physical aspects. For device fabrication the material have strong mechanical property and optical transparency are the important factors for high quality crystals [13-14]. Shimadzu

HMV-2000 tester equipped with a Vickers pyramidal indenter was used to conduct a static indentation test in air at room temperature to measure the microhardness of grown PPN crystal. For all tests, a fixed indentation period (10 s) is used to measure the diagonal length of indentation in m for varied applied weights in kg.



Fi.g.5 plot between Hv Vs load p

The Vickers microhardness values are calculated using the equation,

$$H_v = 1.8544 P/d^2 \text{ kg/mm}^2 \quad (3)$$

where P is the applied load, d is the average diagonal length of the indentation mark and H_v is the Vicker's micro hardness number. The variation of micro hardness number with applied load is plotted in Fig.5. The graph shows that, the hardness increases linearly with the applied load, confirming

the properties of hardness of the crystal. The load and the size of indentations are related through Meyer's law

$$P = k_1 d^n \quad (4)$$

where k_1 is a material constant and n the Meyer's index. Figure 6.6 depicts that the plot against $\log P$ Vs $\log d$. The straight line's slope yields the value of n , which is 2.75.

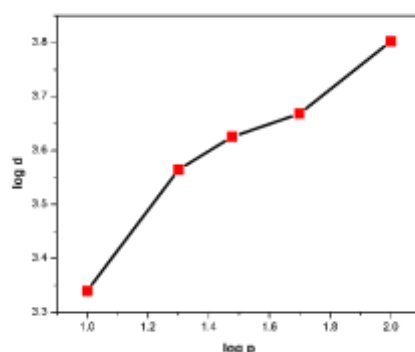


Fig.6 plot between log p Vs log d

According to Onitsch (1947) [15] and Hanneman (1941),[16] "n" should be above 1.6 for softer materials and between 1 and 1.6 for relatively hard materials. Thus, PPN falls within the group of softer materials. Using Wooster's (1953) empirical formula, the elastic stiffness constant is derived by

The stiffness constant's value suggests that the ions are more strongly bound together. The yield

strength σ_v of a material is calculated from the hardness value, using the relation [17]

$$\sigma_v = \frac{Hv}{2.9} \{1 - (n - 2)\}$$

$$2) \left[\frac{12.5(n-2)}{1-(n-2)} \right]^{n-2} \quad (6)$$

Fig 7 shows that the yield strength increases with increasing applied load.

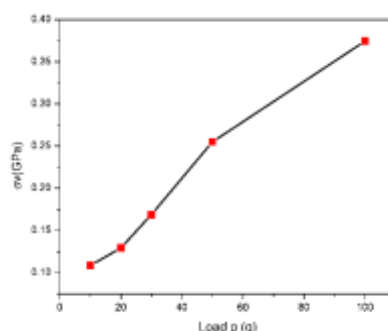


Fig 7 plot between yield strength and load.

The large value of yield strength is due to the tightness of bonding between the atoms. The calculated values of n, yield strength, stiffness

constant and tensile strength are tabulated in table no.2. Thus, the PPN single crystal can be used as the potential and prominent candidate for NLO applications and device fabrication technology.

Table 2. Mechanical parameters of PPN.

Mechanical Parameters	Values
Hardening co-efficient n	2.75
YieldStrength σ_v ($\times 10^8$ Pa)	2.07
StiffnessConstant C_{11} (GPa)	1.46
Tensile Strength T ($\times 10^8$ Pa)	0.90

Thermal Analysis

Differential thermal analysis (DTA) and thermo gravimetric (TG) measurements provide information on phase transition and various stages of crystal decomposition. Fig.8 shows the thermal behavior of the PPN crystal. TG-DTA curves of

grown crystals were recorded in nitrogen atmosphere between 30°C and 500°C. According to TGA curves there is major weight loss from 300°C to 375°C of the crystal, which show that the obtained crystals have no inclusion of solvent and there is no other impurities in the crystal lattices.

The PPN is slightly stable up to 80°C. DTA curve shows sharp endothermic peak observed at 344°C confirming decomposition points of piperazine molecules. The sharpness of the endothermic peaks

indicates that the sample was developed to a high degree of crystallinity.

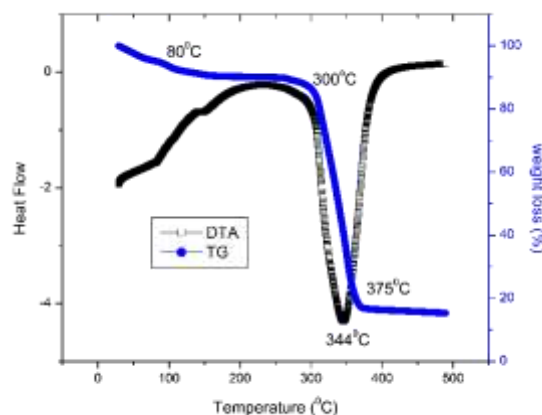


Fig.8 TG-DTA of PPN

Laser damaged threshold studies:

For the optical crystal, laser damage threshold is an important factor affecting its applications in several ways, Lasers can damage transparent optical materials [18]. In this present study, an actively Q-switched Nd: YAG laser was used. The laser was operated at the repetition rate of 10Hz with the pulse duration of 6ns. For the laser damaged threshold measurement the beam was focused on the sample with the focal length of 15cm. during laser radiation, the energy density of the input laser beam for which the crystal being damaged is detected by the power meter. A crack was observed after passing 46 mJ energy in 30s. The energy density is calculated as

$$P = E / \tau \pi r^2$$

(7)

where E is the energy (mJ), τ - pulse width (ns) and r is the radius of the spot (mm). The calculated value of power density for PPS is 9.76GW/cm².

Z-Scan technique:

Z-Scan technique is used to determine the third order nonlinear properties and also find the nonlinear refractive index (n_2), effective nonlinear absorption (β) and optical susceptibility ($\chi^{(3)}$) of

the material. The nonlinear refractive index (n_2), the nonlinear absorption coefficient (β) and the optical nonlinear susceptibility $\chi^{(3)}$ are determined by using closed and open aperture mode Z-scan data [19-20]. A Q-switched Nd: YAG laser having wavelength of 532nm was used as the source of light. In order to transform the input laser beam into Gaussian form, the laser beam was focused using a Gaussian filter. A convex lens (30 mm) was employed to focus the polarised Gaussian beam of mode TEM₀₀, resulting in the beam waist $x_0 = 12.05$ μ m. The sample (L) has a 0.5 mm thickness. The sample was mounted to a holder at a 90° angle and moved in the same direction as the laser beam, which is along the negative (-Z) to positive (+Z) axis. Each movement of the sample table may be managed by a computer. The digital power meter measures the corresponding transmitted intensity via the sample, which was captured by a photo detector. The refractive index of the materials and their degree of absorption has a direct impact on the output intensity of a laser beam. Figures.10 and .11, respectively, depict the PPN crystal's acquired open and closed aperture spectra.

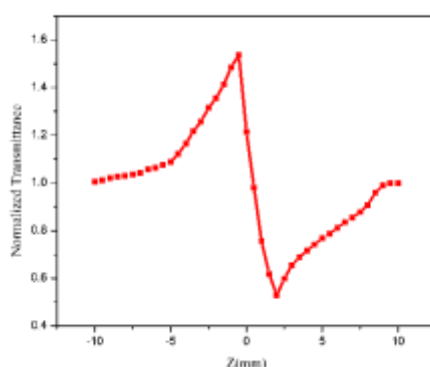


Fig.10 Closed aperture spectrum of PPN single crystal

The nonlinear refractive index of grown crystal was calculated from the closed aperture experiment, the nonlinear refractive index (n_2) of the grown BMZC crystal was calculated using the relation:

$$n_2 = \Delta\phi / k I_0 L_{\text{eff}} \quad (\text{m}^2/\text{W}) \quad (.8)$$

where k is the wavenumber ($k = 2\pi/\lambda$), I_0 is the intensity of the laser beam at the focus ($Z = 0$) and $L_{\text{eff}} = \{[1 - \exp(-\alpha L)]/\alpha\}$ is the effective thickness of the sample, α is the linear absorption and L is the thickness of the sample.

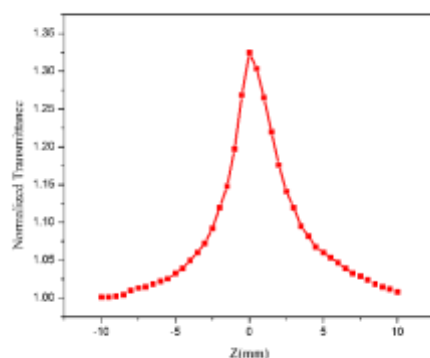


Fig.11 Open aperture spectrum of PPN single crystal

From the open aperture curve, the non-linear absorption coefficient (β) was estimated from the following relation

$$\beta = 2\sqrt{2}\Delta T / I_0 L_{\text{eff}} \quad (9)$$

where ΔT is the peak value at the measured open aperture. The absolute value of the third-order nonlinear optical susceptibility (χ_3) was calculated by using the equation

$$|\chi_3| = [(\text{Re}(\chi_3))^2 + (\text{Im}(\chi_3))^2]^{1/2} \quad (10)$$

where Re and Im are the real and imaginary part of the optical susceptibility. The real and the imaginary parts of the third-order non-linear optical susceptibility (χ_3) were calculated using the following equations

$$\text{Re} \chi_3 \text{ (esu)} = 10^{-4} (\epsilon_0 C^2 n_0^2 n_2) / \pi \quad (\text{cm}^2/\text{w}) \quad (11)$$

and

$$\text{Im} \chi_3 \text{ (esu)} = 10^{-2} (\epsilon_0 C^2 n_0^2 \lambda \beta) / 4\pi^2 \quad (\text{cm}^2/\text{w}) \quad (12)$$

where ϵ_0 is the vacuum permittivity and C is the velocity of light in vacuum. From the Z-scan data, the calculated value of χ_3 is 2.04×10^{-6} esu; n_2 is $4.3 \times 10^{-8} \text{ cm}^2/\text{W}$, $\text{Re} \chi_3$ is 1.51×10^{-6} esu, $\text{Im} \chi_3$ is 1.37×10^{-6} esu and β is $0.22 \times 10^{-4} \text{ m/W}$. Thus, results indicate that PPN crystal has better NLO properties.

3. Conclusion

(10)

Piperazinium Nitrate (PPN) single crystal was grown by slow evaporation technique. Single crystal X-ray diffraction analysis was performed to study the unit cell parameters and space group. The presence of functional groups of the grown PPN crystal was confirmed by using FTIR spectral studies. UV-Vis spectral studies revealed the transparency, cut off wavelength and band gap energy of the grown crystal. Thermal behavior of the grown crystal was using TG/DTA. From the microhardness measurements, it was observed that

the hardness increases with increases of load. The laser damage threshold of grown crystal was found to be 46mJ. The third-order nonlinear optical parameters estimated for grown crystal by Z-scan technique, thus confirms the grown crystal could be used for NLO applications.

4. References

- Yun Zhang, Hua LI, Bin Li, Yunxia Che, Jimin Zheng, 2008, 'Growth and characterization of I histidine nitrate single crystal, apromising semi organic NLO material', *Materials chemistry and physics*, 108, pp.192-195.
- Debrus.S, Ratajczak.H, venturini.J, pincorn.N, Baran.J, Barycki.J, Glowiak.T, pietraszko.A, 2002, 'Novel nonlinear optical crystals of non centrosymmetric structure based on hydrogrn bonds interactions between organic and inorganic molecules', *synthetic Metals*, 127, Pp.99-104.
- johnson.J, Srineeevasn.R and sivavishnu.D, 2018, 'synthesis, growth and charcterisation of dimethylaminopyridine potassium chloride 2-aminopyridine: semiorganic nonlinear optical crystal', *chemistry Reports*, vol.1, pp-20-27.
- franken.A.P, Hill.A.E, Peters.C.W and Weinreich.G, 1961, Generation of optical harmonics, *physical review letters*, 7, pp.118
- T.Kaino,B.Cai,K.Takayama ,2002, Fabrication of DAST Channel Optical Waveguides, *Adv.Funct.Mater.*, Vol.no.12, pp.599–603.
- Sahadevan.K, Narayansamy.D, Kumaresan.P & Anbarasan.P.M, 2016, 'Effect of Swift Heavy Ion Irradiation on Coumarine Doped Glycene Zinc Sulphate (GZS) Semi Organic Crystals for Laser Applications', *International Journal of Advanced Research in Physical Science (IJARPS)*, Volume 3, Issue 1, PP 21-28
- Muthu.K, Meenakshisundaram.S.P, 2012, 'Enhancement of second harmonic generation efficiency: Cs(I)-doped tris(thiourea)zinc(II) sulphate crystals', *J. Phy. and Chem. of Solids*, Volume 73, Issue 9, September 2012, Pages 1146-1150.
- Thomas Joseph Prakash. J, Lawrence.M, 2010, 'Growth and Characterization of Pure and L-lysine Doped Zinc (TRIS) Thiourea Sulphate Crystals', *Int. J. of Comp. Appl.* Volume 8–No.3, pp.36-39.
- Pichan.K, senthil pandian.M, Ramasamy.P, 2017, 'crystal growth and characterization of third order nonlinear optical piperazinium bis (4-hydroxybenzenesulphonate) (P4HBS) single crystal *journal of crystal growth*', vol. 473 pp. 39-54
- Genivaldo Julio Perpe'tuo and Jan Janczak, 2005, 'piperazinium Nitrate, *Acta Crystallographica Section E*', V.61,pp. o2531–o2533.
- John Coates, 2000, 'Encyclopedia of analytical chemistry, John Wiley & sons Ltd, Chichester'.
- Tauc.J, Grigorovici.R, Vancu.A, 1966, 'optical properties and electronic structure of amorphous germanium', *Phys.Status Solidi(B)* vol. 15,pp.627-637.
- Maharani.N.Y, Cyrc Peter.A, Gopinath S. Tamilselvan M. Vimalan I. Vetha Potheher,2016, 'Growth and characterization of amino based organic nonlinear optical L-Lysine-L-Aspartate (LLA) single crystal for electo-optic applications', *J Mater Sci: Mater Electron*, vol.27, pp. 5006-5015.
- Marchewka.M.K, Debrus.S., Ratajczak.H, 2003, 'Vibrational Spectra and Second Harmonic Generation in Molecular Complexes of l-Lysine with l-Tartaric, d,l-Malic, Acetic, Arsenous, and Fumaric Acids, *Cryst.*', *Growth Des.*, Vol.3, pp. 587-594.
- Hanneman M, 1941, *Metall. Manch.* 23 135
- Onitsch E M, 1947 *Mikroscopia*, 2 131
- Mary Linet J, Mary Navis Priya S, Dinakaran S and Jerome Das S, 2008, 'Dielectric and microhardness studies on L-citrulline and L-ascorbic acid admixture TGS crystals', *Cryst. Res. Technol.* Vol. 43, pp. 806
- Nakatani, H, Bosenberg, WR & cheng, LK, 1988, 'Laser induced damage in beta- barium metaborate, *Applied physics Letters*', Vol.53, pp.2587.
- Wang.X.R, Ren.Q, Sun.J, Fan.H.L, Li.T.B, Liu.X.T, Zhang.H.T, Zhu.L.Y, Xu.D, 2011, 'Preparation, crystal growth, characterization, thermal and third-order nonlinear optical Properties of ethyl-triphenyl-phosphonium bis(2-thioxo-1,3-dithiole-4,5-dithiolato) aurate(III) aurate for all-optical switching', *J. Cryst. Growth*, Vol.324, pp. 124–129.
- Deena, S. R., Vickram, S., Manikandan, S., Subbaiya, R., Karmegam, N., Ravindran, B., ... & Awasthi, M. K. (2022). Enhanced biogas production from food waste and activated sludge using advanced techniques—a review. *Bioresource Technology*, 127234.
- Mahapatra, S., Vickram, A. S., Sridharan, T. B., Parameswari, R., & Pathy, M. R. (2016). Screening, production, optimization and characterization of β -glucosidase using microbes from shellfish waste. *3 Biotech*, 6, 1-10.
- Sabari Girisun.T.C, Dhanuskodi.S, Mangalaraj.D, Phillip.J, 2011, 'Synthesis, growth and characterization of bithiourea zinc bromide for optical limiting applications', *Curr. Appl.Phys.*, Vol.11, pp. 838-843.